

# Geophysical Research Letters®

## RESEARCH LETTER

10.1029/2022GL099042

### Key Points:

- Eddy kinetic energy (EKE) is projected to increase throughout the California Current System by the end of the 21st century
- Future changes in EKE are associated with a warmer, more stratified ocean

### Supporting Information:

Supporting Information may be found in the online version of this article.

### Correspondence to:





N. Cordero Quirós,  
[ncorder1@ucsc.edu](mailto:ncorder1@ucsc.edu)

### Citation:

Cordero Quirós, N., Jacox, M. G., Pozo Buil, M., & Bograd, S. J. (2022). Future changes in eddy kinetic energy in the California Current System from dynamically downscaled climate projections. *Geophysical Research Letters*, 49, e2022GL099042. <https://doi.org/10.1029/2022GL099042>

Received 8 JUN 2022  
Accepted 14 OCT 2022

## Future Changes in Eddy Kinetic Energy in the California Current System From Dynamically Downscaled Climate Projections

Nathali Cordero Quirós<sup>1,2</sup> , Michael G. Jacox<sup>1,2,3</sup> , Mercedes Pozo Buil<sup>1,2</sup> , and Steven J. Bograd<sup>1,2</sup> 

<sup>1</sup>Institute of Marine Sciences, University of California, Santa Cruz, CA, USA, <sup>2</sup>Environmental Research Division, Southwest Fisheries Science Center, NOAA, Monterey, CA, USA, <sup>3</sup>Physical Sciences Laboratory, NOAA, Boulder, CO, USA

**Abstract** Eddies in the California Current System (CCS) are generated via baroclinic instabilities of the upwelling jet and contribute to mesoscale variability. However, climate-induced changes in mesoscale activity of the CCS remain poorly explored. We present future eddy kinetic energy (EKE) from an ensemble of three high-resolution downscaled ocean projections covering 1980–2100. EKE is projected to increase throughout the CCS toward the end of the century (2071–2100) compared to a 1980–2010 reference period. Using measures of upper ocean stratification, we find an increasing EKE trend is highly correlated with a more stratified ocean. These findings support previous studies suggesting that mesoscale activity is modulated mainly by baroclinic instabilities, rather than changes in the wind components, which did not show a systematic change across the three projections. Enhanced eddy activity could lead to changes in the distribution and aggregation of biogenic material, having important implications for the CCS.

**Plain Language Summary** The California Current System (CCS) is characterized by seasonal coastal upwelling and energetic currents that have horizontal scales of 10 to a hundred kilometers, referred to as the mesoscale. Together, upwelling and mesoscale activity contribute to a diverse and productive ecosystem. Swirling currents and time varying components of the mesoscale field that occur on time scales of days to months play an important role in distributing ecosystem components. Eddy kinetic energy (EKE) is often used to quantify mesoscale variability and some of the key questions regarding its evolution in a warming ocean still remain poorly addressed. In this study, we use high resolution climate projections of the CCS from 1980 to 2100 to analyze the evolution of EKE. By the end of the century, we find an increase in EKE that is closely related to enhanced stratification of the CCS associated with long-term ocean warming, rather than with changes in the coastal winds and currents. Intensification of eddy activity has important implications for the ecosystem since it significantly influences cross-shore transport of nutrients and other biogenic elements like oxygen, chlorophyll, and planktonic organisms.

## 1. Introduction

The California Current System (CCS) is a highly productive Eastern Boundary Upwelling System (EBUS) that supports important resources such as commercial fisheries and diverse recreational activities along the U.S. West Coast (e.g., Checkley & Barth, 2009; Hickey, 1998; Miller et al., 2015). As in other EBUS, the mechanisms responsible for the high productivity are well understood: the predominantly equatorward wind in this region forces offshore surface Ekman transport, which drives upwelling of nutrient-rich deep waters to the surface near the coastal boundary.

The dynamical field of the CCS is characterized by the presence of a coastal jet that is in geostrophic balance with the upwelled isopycnals alongshore (Castelao & Luo, 2018; Huyer, 1983). Baroclinic instabilities of the upwelling jet generate eddy features such as filaments, cyclones and anticyclones, particularly during the summer and early fall season (Marchesiello et al., 2003; Veneziani et al., 2009). In addition, semi-permanent zonal meanders, extending several hundreds of kilometers offshore, contribute to eddy shedding and therefore to the mesoscale variability and cross-shore transport of biogeochemical properties (Centurioni et al., 2008; Marchesiello & Estrade, 2009; Marchesiello et al., 2003). Eddy features play an important role in the aggregation, transport and dispersion of biogenic material such as chlorophyll, oxygen, and planktonic larvae (Chabert et al., 2021; Davis, 1985; Marchesiello & Estrade, 2009). Moreover, such features have been observed to affect bottom-up

© 2022. The Authors.

This is an open access article under the terms of the [Creative Commons Attribution-NonCommercial-NoDerivs License](https://creativecommons.org/licenses/by-nc-nd/4.0/), which permits use and distribution in any medium, provided the original work is properly cited, the use is non-commercial and no modifications or adaptations are made.

interactions by enhancing energetic transfer within the trophic chain. Coherent eddy structures (such as cyclones or anticyclones) can be hotspots of foraging for top predators since they influence the aggregation of primary producers and consumers (Abrahms et al., 2018; Scales et al., 2018). Taking a closer look into this type of relationships can be beneficial for predicting potential changes in species distribution due to changes in mesoscale activity.

One way of quantifying mesoscale activity is by looking at its signature in eddy kinetic energy (EKE, i.e., the kinetic energy of the time-varying components of the velocity), to which mesoscale eddies are one of the major contributors (Martínez-Moreno et al., 2021; Oliver et al., 2015). While winds drive available potential energy (APE) in coastal regions (Renault et al., 2020), the transformation of APE into EKE occurs mainly via baroclinic instabilities of the coastal upwelling jet. Previous studies have suggested that the wave-like nature of the upwelling front generates instabilities that can amplify even in the absence of external forcing like the wind (Barth, 1989). Marchesiello and Estrade applied a two-layer model in which the upwelling jet of the CCS is scaled in terms of the upwelling of the pycnocline. Their results suggest that the reduced gravity  $g'$  is a good indicator of the velocity shear between two layers, and that stratification dominates the variability of APE for generation of mesoscale activity in the CCS. However, these dynamics have not been explored in the context of a warming ocean under future climate change.

Earth system models (ESMs) are increasingly being applied to understand the evolution of ocean dynamics under future climate scenarios, and these models have shown skill in reproducing physical and biogeochemical patterns in the ocean (e.g., Kwiatkowski et al., 2020). However, the coarse resolution of ESMs limits their ability to reproduce finer scale processes such as upwelling, mesoscale eddy activity, and coastal trapped waves that drive variability in EBUS (Stock et al., 2011). Dynamically downscaled projections combine ESMs and regional models to recover important features that occur at finer scales, allowing study of the response and evolution of regions like the CCS under climate change scenarios (e.g., Auad et al., 2006; Drenkard et al., 2021; Dussin et al., 2019; Howard et al., 2020; Li et al., 2014; Pozo Buil et al., 2021; Xiu et al., 2018). This study leverages an ensemble of dynamically downscaled model projections forced by three different ESMs (Pozo Buil et al., 2021) to explore the changes in EKE and their connection to stratification in the CCS. We first present the changes in the seasonal summer mean (June, July, and August, JJA) of EKE across four selected time periods: 1980–2010 (used as reference), 2011–2040, 2041–2070, and 2071–2100 for each of the three simulations. We then explore the relationship between increasing EKE and enhanced stratification of the upper ocean. Lastly, we discuss the potential implications of increased EKE for the CCS and point to future directions to better understand the links between mesoscale activity and the ecology of the region.

## 2. Methods

### 2.1. Downscaled Climate Projections

To analyze changes in EKE in the CCS, we use an ensemble of high-resolution dynamically downscaled projections from 1980 to 2100. Projections were run using a CCS configuration of the Regional Ocean Model System (ROMS) coupled with a biogeochemical model (ROMS-NEMUCSC) that was forced by three ESMs under the high emissions scenario RCP8.5. The ROMS-NEMUCSC domain extends from 30 to 48°N, covering from mid Baja California to South of Vancouver Island, and from 115.5 to 134°W, with a horizontal resolution of 1/10° (~10 km) and 42 terrain-following vertical levels (Veneziani et al., 2009). The downscaling was performed using a “time-varying delta” method (details in Pozo Buil et al., 2021) to bias correct the atmospheric forcing and lateral ocean boundary conditions derived from the ESMs and used to force the ROMS. This method is described in detail by Pozo Buil et al. (2021), so we provide a brief summary here. First, the time-dependent change (“delta”) from an ESM is calculated by removing its own historical monthly climatology (1980–2010) from the full period of the projection (1980–2100). The change from the ESM is then added to a high-resolution historical climatology derived from atmosphere and ocean reanalyses. In this way, each of the ESM's atmospheric and oceanic forcing fields are bias corrected, while their interannual variability and long-term change are transmitted to the regional model, allowing for simulation of the full transient response (as opposed to a “fixed delta” method that compares discrete future and historical periods). The three ESMs used here were the Geophysical Fluid Dynamics Laboratory's GFDL-ESM2M (Dunne et al., 2012, 2013), the UK Met Office Hadley Center's HadGEM2-ES (Collins et al., 2011), and the Institute Pierre Simon Laplace's IPSL-CM5A-MR (Dufresne et al., 2013). These three ESMs were chosen because they span the CMIP5 range for future physical and biogeochemical changes in

the CCS. Hereafter, we refer to the different downscaled climate projections as ROMS-GFDL, ROMS-HAD, and ROMS-IPSL, respectively.

## 2.2. Eddy Kinetic Energy and Stratification Calculation

We begin by computing the monthly climatology of eastward and northward velocities ( $u$  and  $v$ , respectively) from the three downscaled projections for four different periods: 1980–2010 (reference), 2011–2040, 2041–2070 and 2071–2100. For each period, the monthly climatologies of  $u$  and  $v$  were then subtracted from the daily surface velocity fields to obtain velocity anomalies  $u'$  and  $v'$ , from which daily values of EKE were computed (Equation 1).

$$EKE = \frac{u'^2 + v'^2}{2} \quad (1)$$

We then averaged daily EKE into monthly values to finally compute climatologies of EKE for each of the different periods. Upper ocean stratification was quantified using monthly values of the Brunt-Väisälä frequency ( $N$ , Equation 2)

$$N = \sqrt{-\frac{g}{\rho_o} \frac{\partial \rho(z)}{\partial z}} \quad (2)$$

where  $g$  is the acceleration due to gravity and  $\rho_o$  is the reference density of  $1,027 \text{ kg m}^{-3}$ . For this calculation, the vertical density profile was interpolated to 1 m resolution.  $N$  was calculated at this finer resolution and then averaged over the top 200 m of the water column.

We focus on EKE summer values (JJA) when higher EKE typically occurs (in our simulation and in observations). We also show maps of EKE increase represented by the ratio between the future period of 2071–2100 and the reference period of 1980–2010 ( $EKE_{\text{Future}}/EKE_{\text{Reference}}$ ). Following the idea that density differences between the surface and subsurface layers determine the energy available for EKE conversion via baroclinic instabilities (Barth, 1989, Marchesiello and Estrade), we explore projected changes in density gradients for consistency with changes in EKE. We selected a region defined by  $39\text{--}42^\circ\text{N}$  and  $126\text{--}129^\circ\text{W}$ , where the historical mean EKE is high and all three simulations showed a consistent increase in the future, and calculated the average vertical density gradient for the four selected periods ( $\partial \rho(z)/\partial z$ ).

To capture trends and variability in EKE and stratification across the full spatial domain of the CCS, we calculated empirical orthogonal functions (EOFs) of the monthly EKE and  $N$  fields over the full period (1980–2100) of the simulations. EOFs were calculated separately for EKE and  $N$ , with each spatial EOF pattern having a corresponding principal component (PC) time series. The leading PCs of EKE and  $N$  were low-pass filtered using a Lanczos method with a cut-off frequency of 24 months.

## 3. Results

EKE tends to be higher at locations east of  $\sim 127^\circ\text{W}$ , and this spatial pattern is persistent through the full period of the simulation (1980–2100), though the amplitude is clearly enhanced toward the end of the century. The greatest projected increases of summer EKE occur over an area extending several hundred kilometers offshore in the north and central CCS (Figures 1 and 2), consistent with prior research showing an increase in EKE in the CCS regions east of  $131^\circ\text{W}$  (Xiu et al., 2018). ROMS-HAD shows higher EKE in the regions over the northern part of the domain while ROMS-IPSL and ROMS-GFDL show increases that are more uniform throughout the latitudinal range of the CCS (Figure 1).

By the end of the 21st century, the three downscaled projections show increased EKE in a region that follows the capes and ridges of the coast from north to central CCS ( $48^\circ\text{N}$  down to  $\sim 36^\circ\text{N}$ ), while EKE increases off Point Conception and in the Southern California Bight are relatively weaker. Zonal means of EKE over an area extending 500 km offshore (Figure 1, last column) show that peaks of EKE are located around  $36$  and  $39^\circ\text{N}$ , and that these spots of high EKE are persistent throughout the full simulation (1980–2100).

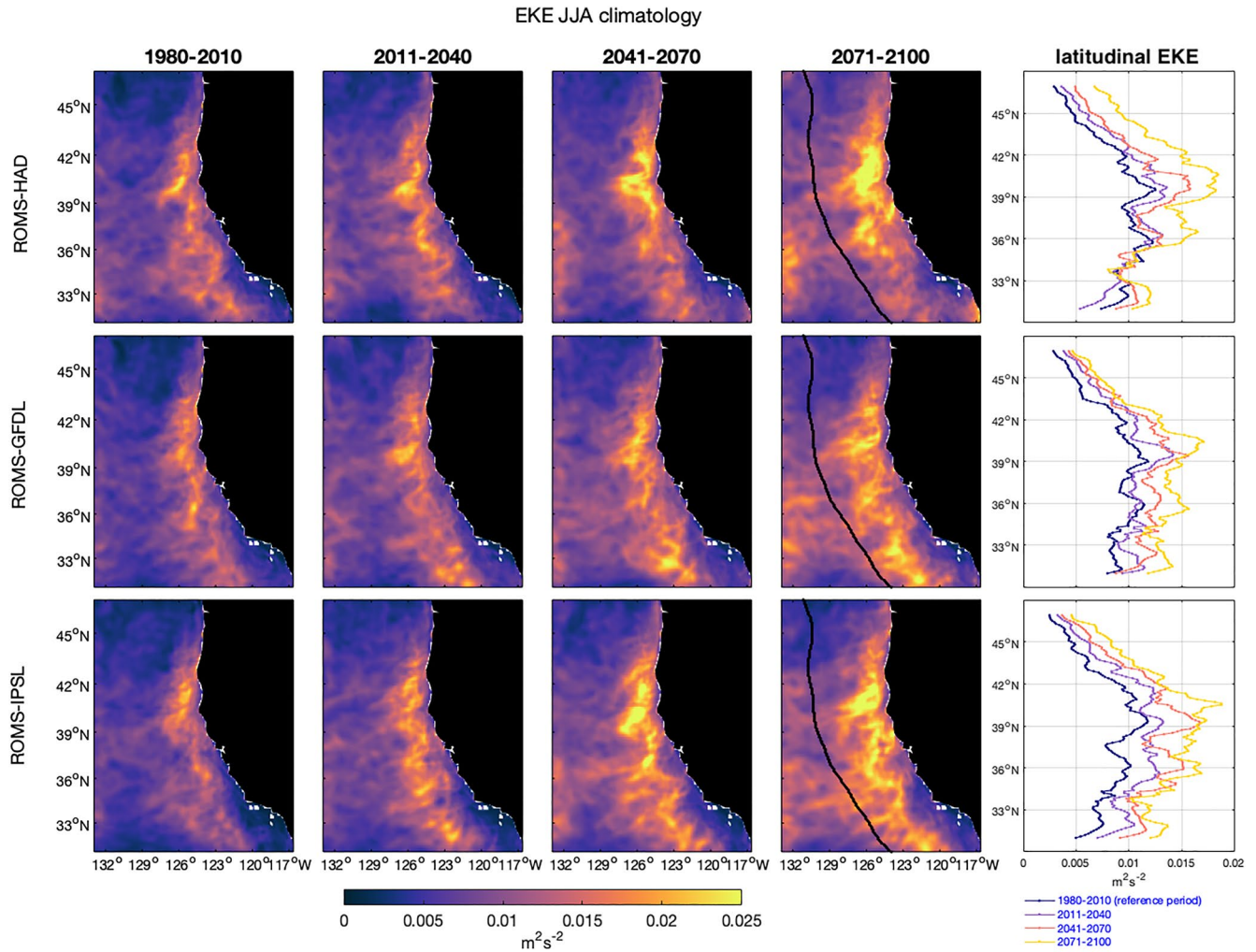


**Figure 1.** Summer (June, July, and August (JJA)) mean eddy kinetic energy (EKE) for the historical period (1980–2010) and three projected periods (2011–2040, 2041–2070, and 2071–2100) for the three downscaled simulations: (top to bottom) regional ocean model system (ROMS)-HAD, ROMS-GFDL, and ROMS-IPSL. Zonal means of EKE from the coast to 500 km offshore (shown by a black contour in the 2071–2100 maps) are shown in the last column.

ROMS-HAD and ROMS-GFDL exhibit strongly enhanced EKE in the northwestern corner of the domain (Figure 2), while the increase in EKE in this region seems to be relatively weaker in ROMS-IPSL. Greater change of EKE in this area is coincident with the region of temperature increase in the open ocean found by Xiu et al. (2018). Pozo Buil et al. (2021) also found a subtle warming in the same northwestern area to be common among the three downscaled projections. Overall, the projected EKE in the future period (2071–2100) consistently increases in all three simulations and in some areas reaches up to five times the EKE in the historical period (1980–2010), particularly north of 39°N (Figure 2).

The three simulations show an increase in the vertical density gradient toward the end of the century (2071–2100) particularly over the upper 200 m of the water column (Figures 3a–3c), indicating a more stratified ocean that is consistent with the surface intensified warming observed in the projections (Pozo Buil et al., 2021). ROMS-HAD and ROMS-IPSL show greater increase in stratification over the whole domain than ROMS-GFDL, indicated by higher vertical density gradients in the future (2071–2100 in Figures 3a–3c) and higher upper ocean buoyancy frequency (Figures 3d–3f).

EOFs are used to capture the domain-wide patterns of both EKE and stratification in the CCS over time. The leading principal components of EKE and buoyancy frequency capture increasing trends over the 21st century (Figure 4). Because stratification is mainly driven by the surface intensified ocean warming, it is not surprising that the variance of the buoyancy frequency is dominated by the warming trend, and the first EOF of buoyancy

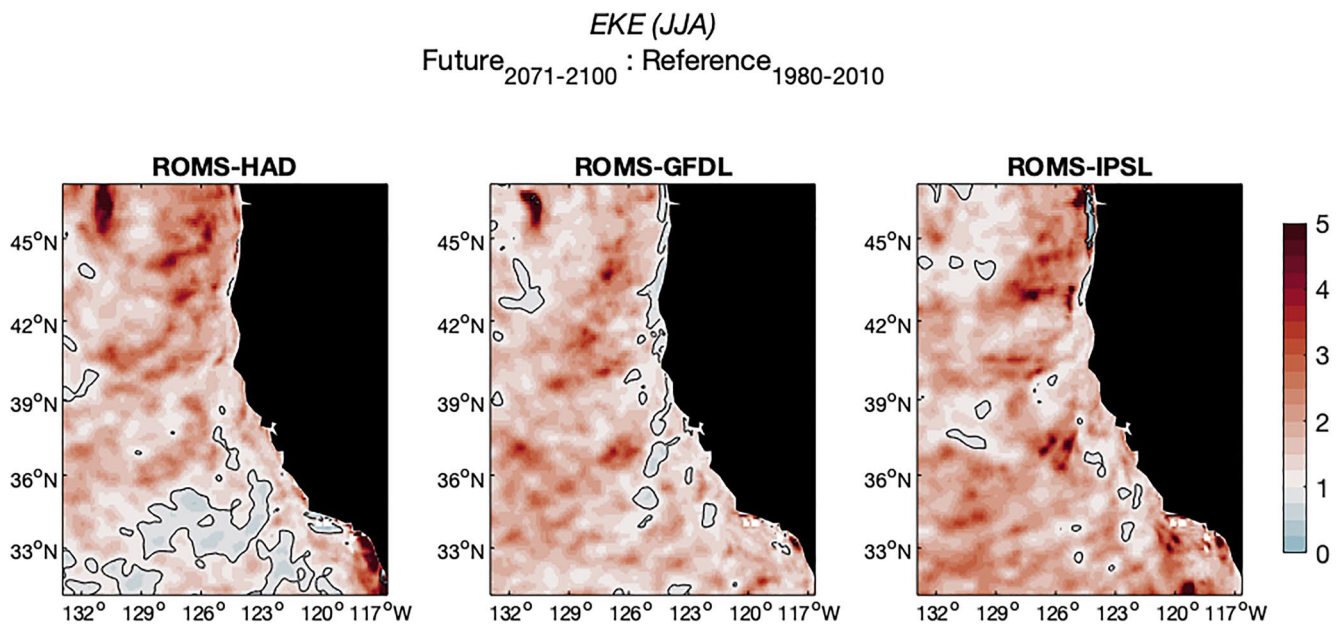


**Figure 2.** Ratio between future (2071–2100) and historical (1980–2010) summer (June, July, and August (JJA)) eddy kinetic energy (EKE) for the three different model projections (left) regional ocean model system (ROMS)-HAD, (middle) ROMS-GFDL, (right) ROMS-IPSL; black contours mark where the ratio equals 1 (i.e., no change).

frequency explains most of the variance in all the three simulations (86% in ROMS-HAD, 84% in ROMS-GFDL, and 87% in ROMS-IPSL). The PC associated with the first EOF of EKE (spatial patterns shown in Figure S4 in Supporting Information S1) captures the low frequency variability of the total EKE fields averaged over the box shown in Figure 4, and it explains 43% in ROMS-HAD and 44% of the variance in both ROMS-GFDL and ROMS-IPSL. Correlations between EKE and N in the three projections are 0.72 (ROMS-HAD), 0.55 (ROMS-GFDL), and 0.76 (ROMS-IPSL). This correlation is consistent with a causative relationship whereby enhanced vertical density gradients drive more EKE through baroclinic instabilities of the upwelling jet. The results suggest that mesoscale activity is likely to increase with a warmer and more stratified CCS.

#### 4. Discussion and Conclusion

Our results show that an increasing trend in EKE in the CCS is highly correlated with increasing stratification due to ocean warming, and that these changes are more coherent during the summer when the mesoscale field in the CCS is more energetic (Figure S1 in Supporting Information S1). This mechanism is not unique to the CCS; in a similar study of the Tasman Sea, Oliver et al. (2015) found that projected EKE increases concurrently with baroclinic and barotropic instabilities of the East Australian Current. It is important to note that even when the initial forcing of the upwelling jet comes from the alongshore (upwelling favorable) winds, the eddy features contributing to variability of the mesoscale field are generated by dynamical (baroclinic) instabilities of such jet. Our analysis suggests that projected future changes in EKE are related mainly to increased upper ocean stratification and not to changes in the wind stress and wind stress curl (Figures S2 and S3 in Supporting Information S1). While increases in EKE and stratification are strong and consistent across all seasons and models, the sign of changes in the wind stress and wind stress curl is dependent on region, season, and model (Figures S2 and S3 in Supporting Information S1), and no systematic change in wind strength was observed. The one consistent response in the projected winds is an increase in wind stress magnitude across much of the domain in spring, which could potentially drive variability in the EKE via an intensified upwelling jet. While our study provides clear evidence for stratification being the dominant driver of future EKE changes in the CCS, further research is necessary to elucidate other mechanisms behind EKE variability and change, such as wind-driven changes in the intensity of the velocities and potential eddy-wind interactions that are not included here (e.g., Renault et al., 2016; Seo et al., 2016).

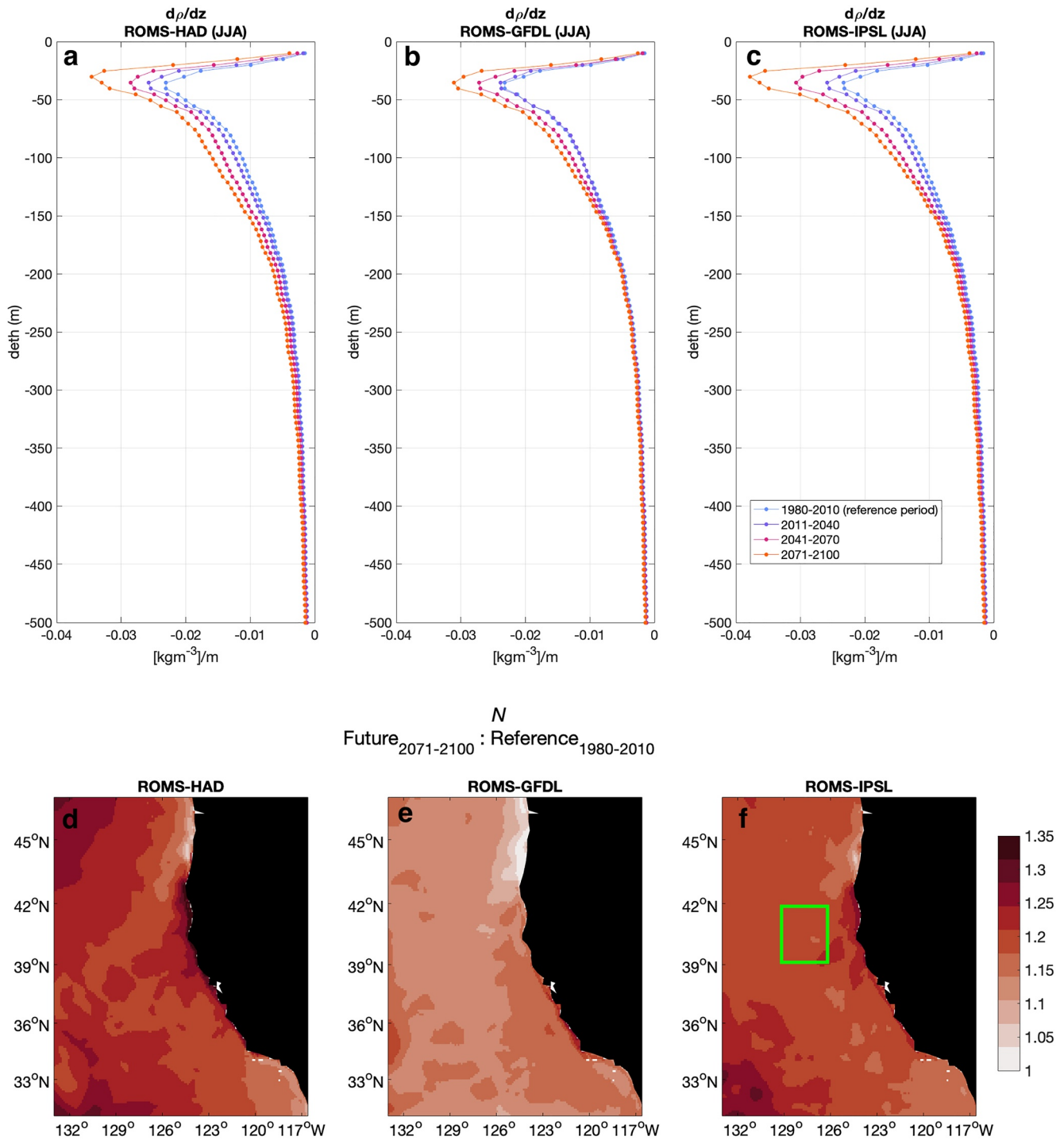


**Figure 3.** (a,b,c) Mean summer (June, July, and August (JJA)) vertical profiles of vertical density gradient averaged over an area defined by 39–42°N and 126–129°W (green box on panel f) for the three different simulations. Different colors indicate the different periods: 1980–2010, 2011–2040, 2041–2070, and 2071–2100. (d,e,f) Increase in stratification as indicated by the ratio of the values of  $N$  in the future divided by the reference period.

Because mesoscale variability plays a key role in the transport and redistribution of biogeochemical properties, it is important to track changes in the mesoscale field and the mechanisms behind such variability. A study by Cheresh and Fiechter (2020) shows that maxima in pH and oxygen values in the nearshore region of the CCS (within ~30 km of shore) are modulated by the meanders associated with the upwelling jet. Their results show maximum values of pH and oxygen during late spring and summer located between 36 and 39°N, corresponding

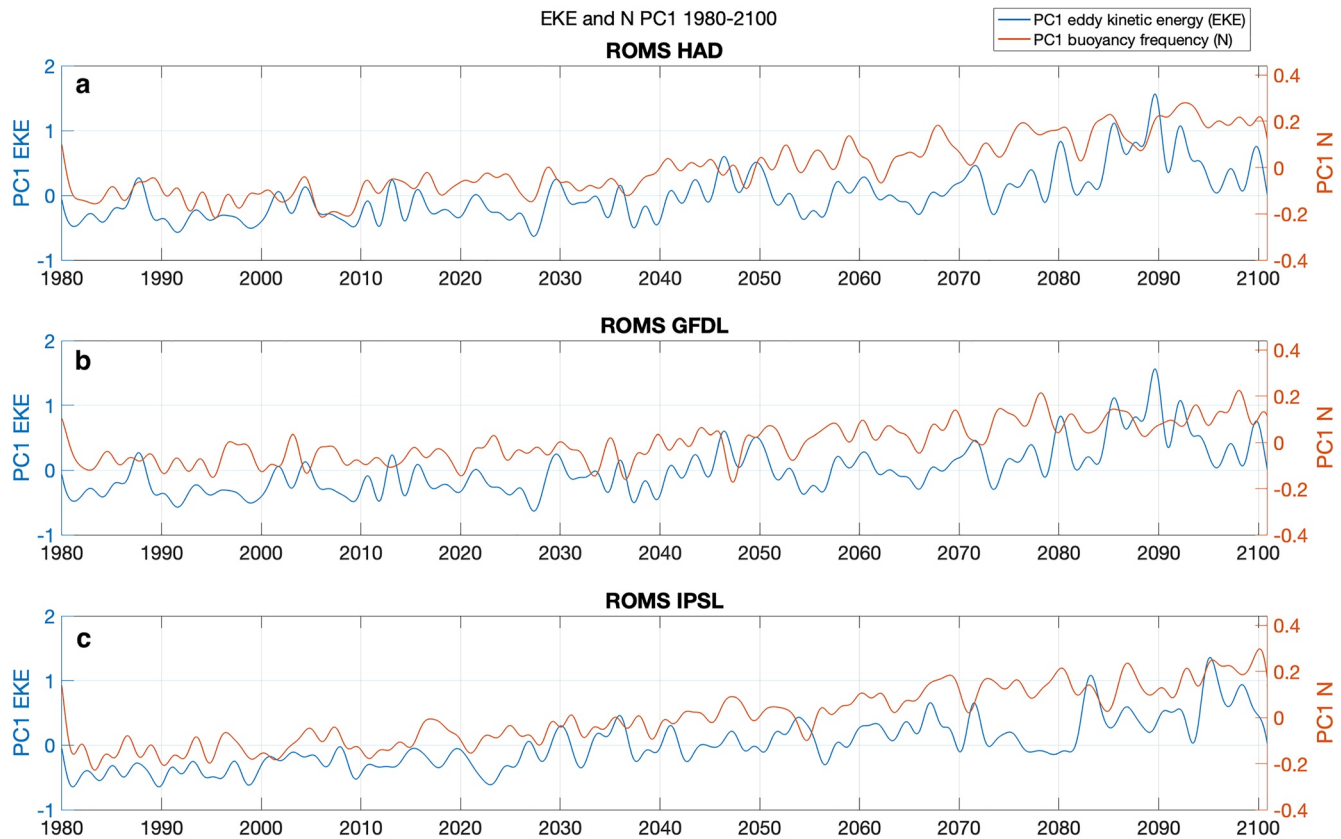


**Figure 4.** Dominant modes of variability in eddy kinetic energy (EKE) (blue) and stratification (orange) for each of the three downscaled projections, as represented by 24-month low-pass filtered principal components (PCs) associated with the first empirical orthogonal function (EOF) of monthly buoyancy frequency and EKE.

with regions of higher EKE (Figure 1). Mesoscale features can also aggregate primary producers, potentially leading to a higher bottom-up energy transfer in the trophic chain (e.g., Abrahms et al., 2018). This aggregation has important implications for the distribution of predatory species such as tunas and sharks, whose foraging habitat has been observed to be influenced by coherent mesoscale eddies and fronts (Braun et al., 2019; Snyder et al., 2017). These studies demonstrate the importance of studying the evolution of the mesoscale field under a changing climate. Future work will investigate whether locations of higher EKE can be linked to hotspots for productivity in the CCS and if these relationships will change in the future.

## Data Availability Statement

Eddy kinetic energy and upper buoyancy frequency projections can be publicly downloaded from the National Oceanographic and Atmospheric Administration's ERDDAP data server at: <https://oceanview.pfeg.noaa.gov/erddap/search/index.html?&searchFor=CCS+ROMS>.

## Acknowledgments

We are grateful for funding from the National Oceanic and Atmospheric Administration Climate Variability and Predictability Program (NA20OAR4310405), the Coastal and Ocean Climate Applications Program (NA17OAR4310268), and the Modeling, Analysis, Predictions and Projections Program (NA20OAR4310447).

## References

- Abrahms, B., Scales, K. L., Hazen, E. L., Bograd, S. J., Schick, R. S., Robinson, P. W., & Costa, D. P. (2018). Mesoscale activity facilitates energy gain in a top predator. *Proceedings of the Royal Society B*, 285(1885), 20181101. <https://doi.org/10.1098/rspb.2018.1101>
- Auad, G., Miller, A., & Di Lorenzo, E. (2006). Long-term forecast of oceanic conditions off California and their biological implications. *Journal of Geophysical Research*, 111(C9), C09008. <https://doi.org/10.1029/2005jc003219>
- Barth, J. A. (1989). Stability of a coastal upwelling front: I. Model development and a stability theorem. *Journal of Geophysical Research*, 94(C8), 10844. <https://doi.org/10.1029/jc094ic08p10844>
- Braun, C. D., Gaube, P., Sinclair-Taylor, T. H., Skomal, G. B., & Thorrold, S. R. (2019). Mesoscale eddies release pelagic sharks from thermal constraints to foraging in the ocean twilight zone. *Proceedings of the National Academy of Sciences*, 116(35), 17187–17192. <https://doi.org/10.1073/pnas.1903067116>
- Castelao, R. M., & Luo, H. (2018). Upwelling jet separation in the California current system. *Scientific Reports*, 8(1), 16004. <https://doi.org/10.1038/s41598-018-34401-y>

- Centurioni, L. R., Ohlmann, J. C., & Niiler, P. P. (2008). Permanent meanders in the California current system. *Journal of Physical Oceanography*, 38(8), 1690–1710. <https://doi.org/10.1175/2008JPO3746.1>
- Chabert, P., d'Ovidio, F., Echevin, V., Stukel, M. R., & Ohman, M. D. (2021). Cross-shore flow and implications for carbon export in the California current ecosystem: A Lagrangian analysis. *Journal of Geophysical Research: Oceans*, 126(2). <https://doi.org/10.1029/2020JC016611>
- Checkley, D. M., & Barth, J. A. (2009). Patterns and processes in the California current system. *Progress in Oceanography*, 83(1–4), 49–64. <https://doi.org/10.1016/j.pocean.2009.07.028>
- Cheresh, J., & Fiechter, J. (2020). Physical and biogeochemical drivers of alongshore pH and oxygen variability in the California current system. *Geophysical Research Letters*, 47(19). <https://doi.org/10.1029/2020GL089553>
- Collins, W. J., Bellouin, N., Doutriaux-Boucher, M., Gedney, A., Alexander, N., Halloran, P., Hinton, T., et al. (2011). Development and evaluation of an Earth-system model – HadGEM2. *Geoscientific Model Development*, 4, 1051–1075. <https://doi.org/10.5194/gmd-4-1051-2011>
- Davis, R. E. (1985). Drifter observations of coastal surface currents during CODE: The method and descriptive view. *Journal of Geophysical Research*, 90(C3), 4741–4755. <https://doi.org/10.1029/jc090ic03p04741>
- Drenkard, E. J., Stock, C., Ross, A. C., Dixon, K. W., Adcroft, A., Alexander, M., et al. (2021). Next-generation regional ocean projections for living marine resource management in a changing climate. *ICES Journal of Marine Science*, 78(6), 1969–1987. <https://doi.org/10.1093/icesjms/fsab100>
- Dufresne, J. L., Foujols, M. A., Denvil, S., Caubel, A., Marti, O., Aumont, O., et al. (2013). Climate change projections using the IPSL-CM5 Earth system model: From CMIP3 to CMIP5. *Climate Dynamics*, 40(9–10), 2123–2165. <https://doi.org/10.1007/s00382-012-1636-1>
- Dunne, J. P., John, J. G., Adcroft, A. J., Griffies, S. M., Hallberg, R. W., Shevliakova, E., et al. (2012). GFDL's ESM2 global coupled climate-carbon Earth system models. Part I: Physical formulation and baseline simulation characteristics. *Journal of Climate*, 25(19), 6646–6665. <https://doi.org/10.1175/jcli-d-11-00560.1>
- Dunne, J. P., John, J. G., Shevliakova, E., Stouffer, R. J., Krasting, J. P., Malyshev, S. L., et al. (2013). GFDL's ESM2 global coupled climate-carbon Earth system models. Part II: Carbon system formulation and baseline simulation characteristics\*. *Journal of Climate*, 26(7), 2247–2267. <https://doi.org/10.1175/jcli-d-12-00150.1>
- Dussin, R., Curchitser, E. N., Stock, C. A., & Van Oostende, N. (2019). Biogeochemical drivers of changing hypoxia in the California current ecosystem. *Deep Sea Research Part II: Topical Studies in Oceanography*, 169, 104590. <https://doi.org/10.1016/j.dsr2.2019.05.013>
- Hickey, B. M. (1998). Coastal oceanography of Western North America from the tip of Baja California to Vancouver Island. In A. R. Robinson & K. H. Brink (Eds.), *The sea, the global coastal ocean: Regional studies and syntheses* (pp. 345–391). J. Wiley and Sons Inc.
- Howard, E. M., Frenzel, H., Kessouri, F., Renault, L., Bianchi, D., McWilliams, J. C., & Deutsch, C. (2020). Attributing causes of future climate change in the California current system with multimodel downscaling. *Global Biogeochemical Cycles*, 34(11), 6646. <https://doi.org/10.1029/2020gb006646>
- Huyer, A. (1983). Coastal upwelling in the California current system. *Progress in Oceanography*, 12(3), 259–284. [https://doi.org/10.1016/0079-6611\(83\)90010-1](https://doi.org/10.1016/0079-6611(83)90010-1)
- Kwiatkowski, L., Torres, O., Bopp, L., Aumont, O., Chamberlain, M., Christian, J. R., et al. (2020). Twenty-first century ocean warming, acidification, deoxygenation, and upper-ocean nutrient and primary production decline from CMIP6 model projections. *Biogeosciences*, 17(13), 3439–3470. <https://doi.org/10.5194/bg-17-3439-2020>
- Li, H., Kanamitsu, M., Hong, S.-Y., Yoshimura, K., Cayan, D. R., Misra, V., & Sun, L. (2014). Projected climate change scenario over California by a regional ocean-atmosphere coupled model system. *Climatic Change*, 122(4), 609–619. <https://doi.org/10.1007/s10584-013-1025-8>
- Marchesiello, P., & Estrade, P. (2009). Eddy activity and mixing in upwelling systems: A comparative study of northwest Africa and California. *International Journal of Earth Sciences*, 98(2), 299–308. <https://doi.org/10.1007/s00531-007-0235-6>
- Marchesiello, P., McWilliams, J. C., & Shchepetkin, A. (2003). Equilibrium structure and dynamics of the California current system.
- Martínez-Moreno, J., Hogg, A. M., England, M. H., Constantinou, N. C., Kiss, A. E., & Morrison, A. K. (2021). Global changes in oceanic mesoscale currents over the satellite altimetry record. *Nature Climate Change*, 11(5), 397–403. <https://doi.org/10.1038/s41558-021-01006-9>
- Miller, A. J., Song, H., & Subramanian, A. C. (2015). The physical oceanographic environment during the CCE-LTER years: Changes in climate and concepts. *Deep-Sea Research*, 112, 6–17. <https://doi.org/10.1016/j.dsr2.2014.01.003>
- Oliver, E. C. J., O'Kane, T. J., & Holbrook, N. J. (2015). Projected changes to Tasman Sea eddies in a future climate. *Journal of Geophysical Research: Oceans*, 120(11), 7150–7165. <https://doi.org/10.1002/2015JC010993>
- Pozo Buil, M., Jacox, M. G., Fiechter, J., Alexander, M. A., Bograd, S. J., Curchitser, E. N., et al. (2021). A dynamically downscaled ensemble of future projections for the California current system. *Frontiers in Marine Science*, 8, 1–18. <https://doi.org/10.3389/fmars.2021.612874>
- Renault, L., McWilliams, J., Jousse, A., Deutsch, C., Frenzel, H., Kessouri, F., & Chen, R. (2020). The physical structure and behavior of the California current system. *BioRxiv*. <https://doi.org/10.1101/2020.02.10.942730>
- Renault, L., Molemaker, M. J., McWilliams, J. C., Shchepetkin, A. F., Lemarié, F., Chelton, D., et al. (2016). Modulation of wind work by oceanic current interaction with the atmosphere. *Journal of Physical Oceanography*, 46(6), 1685–1704. <https://doi.org/10.1175/jpo-d-15-0232.1>
- Scales, K. L., Hazen, E. L., Jacox, M. G., Castruccio, F., Maxwell, S. M., & Lewison, R. L. (2018). Fisheries bycatch risk to marine megafauna is intensified in Lagrangian coherent structures. <https://doi.org/10.1073/pnas.1801270115>
- Seo, H., Miller, A. J., & R Norris, J. (2016). Eddy-wind interaction in the California current system: Dynamics and impacts. *Journal of Physical Oceanography*, 46(2), 439–459. <https://doi.org/10.1175/jpo-d-15-0086.1>
- Snyder, S., Franks, P. J. S., Talley, L. D., Xu, Y., & Kohin, S. (2017). Crossing the line: Tunas actively exploit submesoscale fronts to enhance foraging success. *Limnology and Oceanography Letters*, 2(5), 187–194. <https://doi.org/10.1002/lol2.10049>
- Stock, C. A., Alexander, M. A., Bond, N. A., Brander, K. M., Cheung, W. W. L., Curchitser, E. N., et al. (2011). On the use of IPCC-class models to assess the impact of climate on living marine resources. *Progress in Oceanography*, 88(1–4), 1–27. <https://doi.org/10.1016/j.pocean.2010.09.001>
- Veneziani, M., Edwards, C. A., Doyle, J. D., & Foley, D. (2009). A central California coastal ocean modeling study: 1. Forward model and the influence of realistic versus climatological forcing. *Journal of Geophysical Research*, 114(C4), 4774. <https://doi.org/10.1029/2008jc004774>
- Xiu, P., Chai, F., Curchitser, E. N., & Castruccio, F. S. (2018). Future changes in coastal upwelling ecosystems with global warming: The case of the California current system. *Scientific Reports*, 8(1), 2866. <https://doi.org/10.1038/s41598-018-21247-7>